The Journal of Chemical Physics

AIP Publishing

Rotational Investigations of Volatile Anesthetics: Conformational Equilibrium, Molecular Structure and Complex Hyperfine Interactions of Methoxyflurane

Sven Herbers,[1,a)] Wenqin Li,[2] Philipp Buschmann,[3] Meng Li,[3] Jens-Uwe Grabow,[3,a)] Alberto Lesarri[2,a)]

[1]*Laboratoire Inter-Universitaire des Systémes Atmospheriques (LISA) - UMR CNRS 7583, Université Paris-Est Créteil, 94010 Créteil, France*

[2]*Departamento de Química Física y Química Inorgánica, Facultad de Ciencias – I.U. CINQUIMA, Universidad de Valladolid, Paseo de Belén, 7, 47011 Valladolid, Spain*

[3] *Institut für Physikalische Chemie und Elektrochemie, Gottfried-Wilhelm-Leibniz-Universität Hannover, Callinstrasse 3A, 30167 Hannover, Germany*

a) Authors to whom correspondence should be addressed: sven_herbers@web.de, jens-uwe.grabow@pci.uni-hannover.de, alberto.lesarri@uva.es

ABSTRACT

The volatile anesthetic methoxyflurane was investigated in the 2 to 8 GHz region by chirp-excitation Fourier-Transform broadband microwave spectroscopy. The presence of two conformers — *gauche-trans* (C_1) and *trans-trans* (C_S) — each containing two quadrupolar chlorine nuclei and one methyl internal rotor, results in a dense spectrum with complex rotational hyperfine effects, where contributions from nuclear quadrupole interactions and internal rotation couple to the overall molecular rotation. For the more complicated C_1-conformer, additional impulse-excitation cavity measurements were carried out in the region of 10 to 21 GHz. To the best of our knowledge there is no published code that can handle two quadrupolar nuclei in a non-coplanar orientation with respect to the internal rotor, so we developed our own codes interfacing with Pickett's *SPFIT* rovibrational fitting program to allow for a near-experimental accuracy fit of the relatively abundant isotopologues, comprising all isotopologue combinations of the ^{35}Cl and ^{37}Cl nuclei. Furthermore, the Hartwig-Herbers' *XIAM-NQ* code was later extended to treat a second quadrupolar nucleus, and global fits with this new code *XIAM-2NQ* were validated against *SPFIT* results. The relative transition intensities of the two conformers were used to estimate the relative room-temperature population as $N(C_s)/N(C_1) = 0.88 \pm 0.30$ corresponding to a difference in the Gibbs free energy of $\Delta G^{\ominus}_{\mathrm{m,298K}} \approx$ -1.4 ±1.1 kJ/mol. A computational characterization using density functional theory (CAM-B3LYP-D3(BJ)) complemented the experimental results. This work completes the rotational investigations on the conformational and structural panorama of the most important halogenated inhalational anesthetics, potentially enabling their monitoring through distinct spectroscopic fingerprints.

I. INTRODUCTION

General anesthetics attract permanent interest for fundamental, biochemical, and medical reasons. Paradoxically, anesthetic molecules are chemically very diverse, including, among others, mono- and diatomic gases, ethers, phenols, barbiturates, and steroids. The pharmacological effects, expressed in terms of potency range, offer a large variability and span several orders of magnitude. For these reasons, the molecular mechanisms underlying chemically-induced loss of consciousness still remain debatable to this date.[1–3] Anesthetics are expected to bind to specific protein targets in the central nervous system, modulating neuronal pathways. [4,5,6,7] However, high-resolution diffraction studies of anesthetic binding sites are limited to soluble proteins.[8,9] From a technological point of view, the molecule-specific rotational signatures could potentially be used to detect or quantify the presence of anesthetics in a gas mixture or *in vivo*. Up to date rotational spectra have been obtained for different general and local anesthetics including polyfluorinated ethers (sevoflurane,[10] isoflurane,[11] desflurane,[12] enflurane[13] and fluoroxene[14]), phenol derivatives (propofol[15]), and aminobenzoates (benzocaine[16]).

Among the inhalational anesthetics, many halogenated hydrocarbons were tested for clinical use since the 1950's [17] (Figure 1), and two of them (isoflurane and sevoflurane) remain in the World Health Organization Model List of Essential Medicines. Some other compounds have been phased out or are used for specific purposes. Methoxyflurane (Penthrane ®, 2,2-dichloro-1,1-difluoroethyl methyl ether or $CHCl_2CF_2OCH_3$), first introduced for general anesthesia in 1962 as non-toxic replacement for halothane,[18] was retired in the late 1970s because of dose-related nephrotoxicity[19] and is now used only in some countries for trauma and acute pain relief.[20] While other inhalational anesthetics could be analyzed rotationally,[10-14] methoxyflurane was only investigated in low resolution with IR and Raman spectra, along with a microwave band spectrum presented by Durig.[21] Due to their low resolution, the rotational analysis in this study was limited to a rough estimate of the sum of rotational constants *B* and *C* (2036 MHz) and the realization that likely two conformers contributed to the spectrum.

Methoxyflurane exhibits two chlorine nuclei with a spin of $I = 3/2$, each occurring either as ^{35}Cl (76%) or ^{37}Cl (24%), and a methyl group attached to the ether oxygen. Because of the anticipated presence of two conformers, the various isotopologues, the nuclear quadrupole coupling of the ^{35}Cl and ^{37}Cl nuclei, and a barrier hindering the methyl internal rotation of only about 336 cm^{-1} (ca. 4.02 kJ mol^{-1}, as observed for the similar methyl group in methoxynonafluorobutane,[22] (*n*-$C_4F_9OCH_3$)), the molecule is expected to display very complicated spectral fine and hyperfine structures, rendering the rotational analysis extremely difficult. Moreover, methodological difficulties exist in expressing a rotational

Hamiltonian which includes the coupling of the spins of the two quadrupolar nuclei, the internal rotation of the methyl group, and the overall rotation of the molecule. For this reason, currently used computer codes for internal rotation provide only an approximate treatment of nuclear quadrupole coupling. An example is the application of Kleiner's *BELGI-2N* code to methylimidazole.[23] Recently, there were some developments in the extension of internal rotation codes, giving rise to Westerfield's new *westerfit* program,[24] which currently handles C_s-symmetric molecules with internal rotation and quadrupole coupling, and a modification of Hartwig-Herbers' *XIAM*, called *XIAM-NQ*,[25] which treats the quadrupole coupling of one nucleus exactly. However, the successful treatment of experimental spectra showing quadrupole coupling of multiple nuclei in combination with internal rotation in C_1-symmetric molecules has, to this date, not been demonstrated. In this work, we exploited the broad bandwidth and dynamic range of chirped-pulse microwave excitation[12,26] to resolve the rotational spectrum of methoxyflurane. In addition, different strategies for fitting and analyzing the molecule will be discussed, which could be applied to related molecules with complex hyperfine patterns associated with multiple nuclear quadrupole couplings and internal rotors. Furthermore, we introduce an extended version of *XIAM-NQ*, referred to as *XIAM-2NQ*, which can handle two quadrupolar nuclei ($I > 1/2$) and internal rotation in molecules even in absence of symmetry (C_1 point group). This new implementation is demonstrated to achieve experimental accuracy in spectral fits of methoxyflurane. The study completes the conformational and structural panorama of the most important inhalational anesthetics, providing a unified molecular description of this series of biologically relevant compounds.

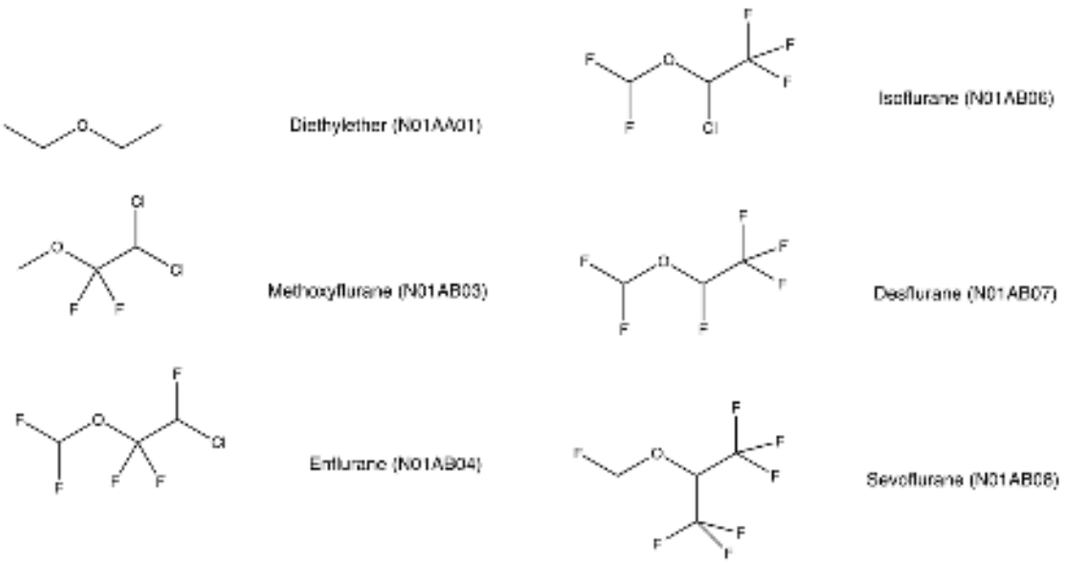

Fig. 1. Diethyl ether and several halogenated ethers used for inhalational general anesthesia (Anatomical Therapeutical Chemical or ATC codes in parentheses).

II. EXPERIMENTAL AND COMPUTATIONAL METHODS

Methoxyflurane is liquid at room temperature (m.p. 237 K, b.p. 378 K) and was obtained commercially (97%). For the broadband experiments in the 2-8 GHz region, the sample was placed at room temperature in the liquid reservoir of two solenoid injectors (Parker series 9), separated 25 cm and equipped with circular orifice nozzles (orifice diameter 1 mm). A molecular jet was generated by co-expanding the sample's vapor with a mixture of Argon and Helium (1:1) at 3 bar into the spectrometer chamber, evacuated to ca. 10^{-6} mbar with two diffusion pumps backed by roots and rotary pumps. The microwave spectrometer in Valladolid is based on a 25 GSample/s arbitrary waveform generator, creating chirps of 4 μs duration from 2 to 8 GHz. Following amplification with a 250 W travelling-wave tube power amplifier, the excitation radiation is broadcasted perpendicularly to the molecular jet using a horn antenna. The receiver consists of a second colinear antenna and a low-noise amplifier, prior to a 25 GSample/s digital oscilloscope, which records the free-induction decay (FID) of the molecular emission for periods of 40 μs. The present experiment included 800,000 averages, exercising eight chirp excitations on each gas injection. Fourier transformation was used to convert the time-domain recording into the frequency-domain spectrum. Transition frequencies were determined with an accuracy better than 10 kHz.

Due to the inequivalence of the quadrupolar nuclei, the number of independent quadrupolar coupling parameters is significantly higher for the C_1-conformer (10) than for the C_S-conformer (5). To achieve good fitting results for the complete quadrupole coupling symmetric traceless tensors of the most abundant isotopologue of the C_1-conformer, more data were required, and additional impulse-excitation resonator-enhanced measurements were conducted in the 10 to 21 GHz range. The spectra were recorded at room temperature in Hannover, using the coaxially oriented beam resonator arrangement Fourier transform microwave (COBRA-FTMW) spectrometer.[27] Neon was used as the carrier gas at a stagnation pressure of approximately 2 bar before being supersonically expanded into the vacuum chamber (~10^{-5} mbar during the experiment) through a solenoid valve (Parker, General Valve Series 9, circular nozzle orifice diameter 0.5 mm). All transitions appear as Doppler-split pairs because the coherently rotating ensemble of molecules emits both parallel and anti-parallel to the propagation direction of the molecular jet with both components detected.

Several quantum chemical methods complemented the experiments, including MP2 second-order perturbation theory and density functional methods. We report the results obtained with the hybrid CAM-

B3LYP functional using the Coulomb-attenuating method of Yanai,[28] supplemented with the D3 empirical dispersion term of Grimme with Becke-Johnson (BJ) damping.[29–31] The calculations were performed using the aug-cc-pVTZ (aVTZ) augmented correlation-consistent triple-ζ basis set[32] as implemented in Gaussian16.[33]

III. RESULTS

Computational predictions initially suggested two predominantly populated conformers of methoxyflurane: a *trans-trans* plane-symmetric structure (C_S) and a *gauche-trans* asymmetric (C_1) structure (Figure 2). With inclusion of anharmonic frequency calculations and zero-point vibrational energies, these conformers are predicted to be isoenergetic (within 0.01 kJ/mol), leaving unclear which of the two conformers is more stable.

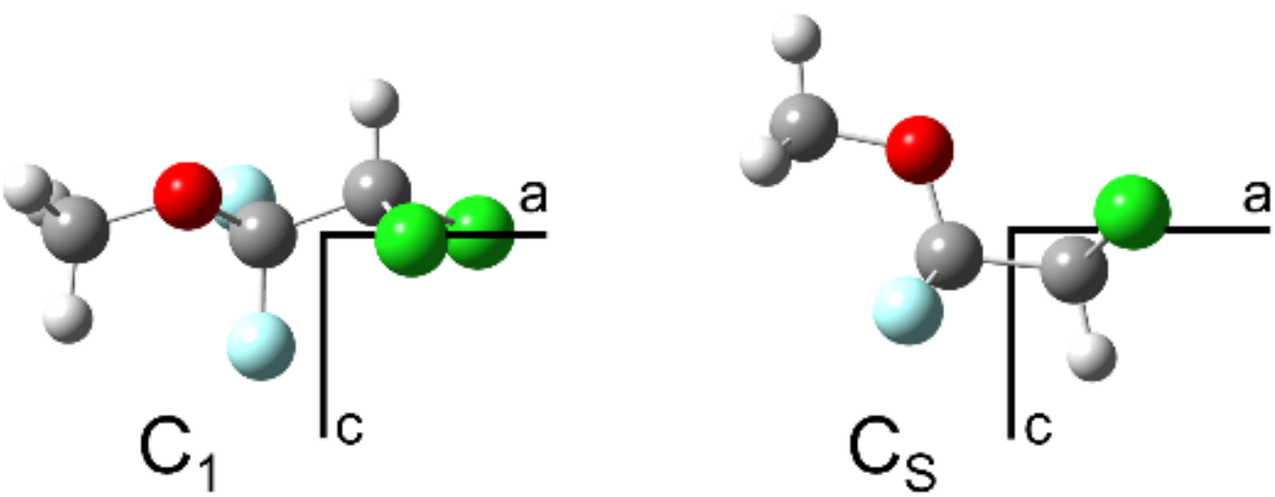

Fig. 2. Methoxyflurane in its principal inertial axis system, view along the *b*-axis (perpendicular to the Figure). Left panel: *gauche-trans* C_1-conformer. Right panel: *trans-trans* C_s-conformer.

Both of the predicted conformers were identified by their spectral signatures in the broadband spectrum of Figure 2. For each conformer, the various ^{35}Cl and ^{37}Cl isotopologues were observed in natural abundance (ca. 75.8% and 24.2% for the single isotope). On top of the plethora of transitions originating from the various isotopologues, there are splittings originating from the nuclear quadrupole coupling of the chlorine nuclei and the internal rotation of the methyl group, also illustrated in Figure 3. Including the resonator measurements, a total of 3014 transition lines were measured. By applying reasonable intensity and frequency cutoffs, 2918 of these signals could be tentatively assigned to one of the isotopologues of one of the conformers of methoxyflurane. A set of 96 signals remain unassigned, initially suspected to have their origin in GSM signals, interfering with the experiment at around 2110-2140 MHz. Of the 2918 tentative assignments, 2367 belonged to the C_1-conformer, while the remaining 551 belonged to the C_s conformer. Blended signals, lines at low signal-to-noise ratio, or transitions with ambiguous assignment were not included in the final fits. A total of 1428 lines were used in the fits of the C_1-conformer's isotopologues, while a total of 439 transitions were used in the fits of the C_s-conformer's isotopologues. More details on the complete line list and assignments to isotopologues can be found in the supplementary material.

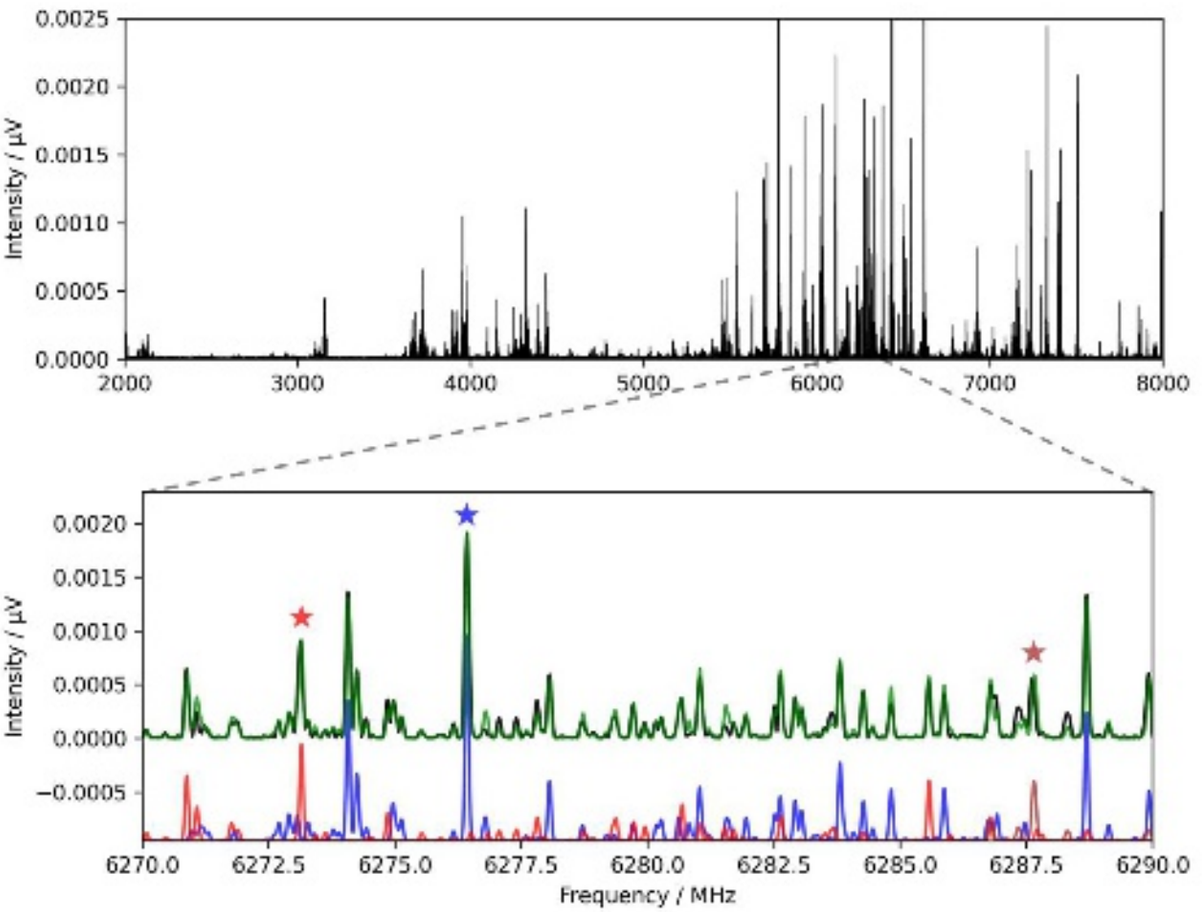

Fig. 3. Upper panel: Global view of broadband chirp-pulse FTMW rotational spectrum of methoxyflurane. Lower panel: Section covering most of the $J'_{K'_a,K'_c} - J''_{K''_a,K''_c} = 3_{2,1}{-}2_{2,0}$ quadrupole coupling and internal rotation pattern of the C_1-symmetric conformer (^{35}Cl-^{35}Cl isotopologue), together with simulations of the internal rotation *A* (blue) and *E* (red) symmetry species (negative offset added for clarity). Overlapping parts of the $3_{1,2}{-}2_{1,1}$ transition of the ^{37}Cl-^{37}Cl isotopologue are indicated in the brown trace. Combination of all predicted spectra results in the total simulated spectrum (green). The *A* and *E* species transitions as well as the ^{37}Cl-^{37}Cl isotopologue predictions are each scaled to the respective peak marked with an asterisk.

The *SPFIT/SPCAT* rovibrational fitting codes from Pickett's CALPGM suite of programs[34] were used to carry out the first spectral fits/predictions. The general semi-rigid rotor treatment,[35] nuclear quadrupole coupling[36] and (local) internal rotation treatment,[37] are described in more detail in the supplemental material, as well as the respective literature. *SPFIT* has limitations in its implementation of the complete Hamiltonian, not allowing for all internal rotation parameters (D_a, D_b, D_c) and quadrupole coupling tensor off-diagonal elements ($\chi_{ab}, \chi_{ac}, \chi_{bc}$) to be fitted at the same time. A two-step procedure was then applied: First, we fitted only the *A*-symmetry species with a complete Hamiltonian, not requiring $D_a, D_b,$ or D_c. The effect of the off-diagonal elements of $\boldsymbol{\chi}$ on the spectral

lines was then calculated for the *A* species, subsequently correcting the *A* species as well as the *E* species for this effect. In a second fit, the Hamiltonian was set up to include the *A* and *E* species, the internal rotation parameters of the *E* species D_a, D_b, D_c but no off-diagonal elements of $\boldsymbol{\chi}$. Applying the corrections from the first step, near experimental accuracy fits (about 10 kHz) could be achieved this way, with errors due to the two-step approximation estimated to be on the order of 3 kHz. The internal rotation programs *XIAM*[38] as well as *Mathieu*[39] were used to derive internal rotation parameters. With the initial fits in place, a sufficiently large enough dataset for methoxyflurane was available to attempt an extension of the recently published *XIAM-NQ*[25] version from one to two quadrupolar nuclei, becoming *XIAM-2NQ*. From equations (1), (3), (4), (5), (8), and (10) of Ref.[36] the general quadrupole coupling matrix elements of the *L*-th of *N* nuclei can be derived. For the elements of the first and second nucleus one obtains specifically

$$\left(J, K, I_1, F_1 \middle| H_{Q_1} \middle| J', K', I_1, F_1\right) = (-1)^{t_1} \begin{Bmatrix} F_1 & I_1 & J \\ 2 & J' & {I_1}' \end{Bmatrix} [(2J+1)(2J'+1)]^{1/2} \frac{\begin{pmatrix} J & 2 & J' \\ -K & -q & K' \end{pmatrix}}{\begin{pmatrix} I_1 & 2 & I_1 \\ -I_1 & 0 & I_1 \end{pmatrix}} \chi_{1,-q}/4 \tag{1}$$

with

$$t_1 = J + K + I_1 + J' + F_1 + 1 \tag{2}$$

and

$$\begin{aligned} \left(J, K, I_1, F_1, I_2, F \middle| H_{Q_2} \middle| J', K', I_1, F_1', I_2, F\right) = \\ (-1)^{t_2} \begin{Bmatrix} F & I_2 & F_1 \\ 2 & {F_1}' & {I_2}' \end{Bmatrix} [(2F_1+1)(2F_1'+1)]^{\frac{1}{2}} \begin{Bmatrix} J & F_1 & I_1 \\ F_1' & J' & 2 \end{Bmatrix} \\ \times [(2J+1)(2J'+1)]^{1/2} \frac{\begin{pmatrix} J & 2 & J' \\ -K & -q & K' \end{pmatrix}}{\begin{pmatrix} I_2 & 2 & I_2 \\ -I_2 & 0 & I_2 \end{pmatrix}} \chi_{2,-q}/4 \end{aligned} \tag{3}$$

with

$$t_2 = K + I_1 + I_2 + 2F_1' + F + 1. \tag{4}$$

Here the 2×3 expressions in parentheses are Wigner-3j symbols and the 2×3 expressions in curly brackets are Wigner-6j symbols. Efficient FORTRAN evaluation routines for these symbols are publicly available.[40] These routines and matrix elements were implemented into the new *XIAM-2NQ* code,[25] and

global fits without the two-step approximation with *SPFIT/SPCAT* were possible. These *XIAM-2NQ* fits converged to about 9 kHz and generally showed slightly better root-mean-square deviations (σ) while using less parameters. All necessary input and output files for all isotopologues of both conformers are available in the supplementary material.

With respect to the assignment process, *XIAM-2NQ* chooses the *J* quantum number as the one with the highest contribution to the state vector. In contrast, for the bad F_1 quantum number, the assigned value may not correspond to a single dominant contribution, and multiple state vectors are compared to find the best mutual assignments.

While the fits with *XIAM-2NQ* are more accurate than the *SPFIT* method described here, intensity predictions are only implemented with the coarse approximation that there are no cross-*J* transitions, and that F_1 is a nearly-good quantum number, which especially for the *Cs* conformer with equivalent nuclei leads to large errors in predicted intensities. Consequently, for quantitative intensity comparisons it is recommended to use *SPCAT* instead. More information on the *XIAM-2NQ* extension can be found on the associated github site.[41] In Figure 3, a section of the broadband spectrum around the $J'_{K_a',K_c'} - J''_{K_a'',K_c''} = 3_{2,1}-2_{2,0}$ transition of the C_1-conformer illustrates the quality of the fit, which is compared with simulations based on *SPCAT* predictions.

The results for the $^{35}Cl,^{35}Cl$ isotopologues of the C_1- and the C_s-conformer are provided in Table 1 while the other combinations of chlorine isotopes are summarized in the supplementary material. The determined barriers to the methyl group internal rotation of 350 cm^{-1} and 336 cm^{-1} agrees well with the barrier of 336 cm^{-1} found in n-$C_4F_9OCH_3$,[22] which features a methoxy-methyl group in a near-identical electronic environment connected via the oxygen to an difluoromethylene -CF_2- carbon. This highlights the fact that barriers for similar environments can be partially categorized, and this allowed for a precise initial prediction during our assignment process. Relative intensities were determined from the experimental spectrum within the center portion from 4 to 6 GHz, to reduce uncertainties associated to instrumental factor. The population ratio in the jet was then calculated as $\frac{N_{Cs}}{NC_1} = 0.88 \pm 0.30$ under the assumption of a quadratic dependence with the electric dipole moment.[42] The error on the population ratio was estimated from the comparison of different intensity ratios and includes an additional 10% uncertainty attributed to estimated errors in the dipole moments, with more details provided in the supplementary material. Despite the large error bar, all estimates yield $\frac{N_{Cs}}{NC_1}$>0.5, implying that the C_s

conformer is preferred. In order to obtain the Gibbs free energy, we further assumed that the relative populations after the molecular jet expansion are determined by the pre-expansion room temperature, which leads to a difference in Gibbs free energy of $\Delta G^{\ominus}_{\mathrm{m,298K}} = -1.4 \pm 1.1$ kJ/mol. On the other hand, the Gibbs free energy was computed as 1.01 kJ/mol. Taking into account the two-fold degeneracy of the C_1-conformer a population ratio of $\frac{N_{Cs}}{NC_1}$ =0.33 could be predicted. While this result does not agree well with our experimental estimate, it is important to consider that the relative energies are very small, and at the chosen quantum chemical level, errors on the order of a few kJ/mol are perfectly reasonable. In fact, merely switching between the harmonic and anharmonic treatments of vibrations alters the quantum chemically predicted Gibbs free energy. The previously anharmonic value shifts to $\Delta G^{\ominus}_{\mathrm{m,298K}} =$ -0.02 kJ/mol, with a corresponding population ratio of $\frac{N_{Cs}}{NC_1}$ =0.50 in the harmonic case. Therefore, we expect our experimental values to be more accurate. However, it should be emphasized that both the magnitude and associated errors are based on estimates and should be interpreted with caution. In particular, the relative intensities used are influenced by several unnormalized instrumental factors, such as power fluctuations and other systematic variations.

The assumption that relative populations in the jet are determined by the pre-expansion equilibrium values is not valid in the case of collision-induced conformational relaxation. Moreover, conformational temperatures have been observed to be much smaller than room temperature in some multi-conformational systems. As an example, in hexanal[43] the observed conformational temperature was 135 K. Since conformational relaxation critically depends on the interconversion barrier, we additionally examined the torsional potential energy surface of methoxyflurane. The results from the relaxed potential energy scan in Figure 4 suggests large interconversion barriers exceeding 1500 cm^{-1}, much larger than the empirical interconversion threshold barriers[44] of 400 cm^{-1}. The axis of Figure 4 representing the dihedral angle corresponding to the terminal dichloromethyl –$CHCl_2$ group starts with -180°, corresponding to the equilibrium structure of the *gauche-trans* C_1-conformer. The first barrier shown in Figure 4 is encountered at -120° and it separates the two equivalent C_1-conformers with a value of about 1700 cm^{-1}. The local minimum at about -60° is the second C_1-enantiomer. The barrier at 0° and 120° corresponds to the barrier separating C_1- from C_S-conformer with a value of about 1900 cm^{-1}. The local minimum at about 60° is the C_S-conformer. Even at room temperature only about 0.1% of molecules have kinetic energies on the order of 1900 cm^{-1}, according to the Maxwell-Boltzmann distribution, meaning that the assumption of the relative populations of *trans-trans* C_S and *gauche-trans* C_1

conformers being 'frozen' on the room temperature values throughout the jet expansion is reasonable and no relaxation is expected between the C_1- and C_S-conformers of methoxyflurane.

Table I. Experimental molecular parameters from spectral fit of the ^{35}Cl-^{35}Cl major isotopologue of methoxyflurane compared to quantum chemical predictions using anharmonic frequency calculations with CAM-B3LYP-D3BJ/aVTZ as implemented in Gaussian16. For A_0, B_0, C_0 of *SPFIT* the approximation B_0=(1/3 B_A + 2/3 ΔB_E) was applied, which is generally valid for V_3 barriers of several hundreds of wavenumbers.

	Gauche-Trans C_1-Conformer			*Trans-Trans* C_S-Conformer		
Parameter / MHz	Experiment *SPFIT*	Experiment *XIAM-2NQ*	CAM-B3LYP-D3BJ/aVTZ	Experiment *SPFIT*	Experiment *XIAM-2NQ*	CAM-B3LYP-D3BJ/aVTZ
A_e			1994.971			1791.280
B_e			1155.680			1166.522
C_e			853.079			931.705
A_A	2002.45376(38)			1795.961(10)		
B_A	1155.654827(79)			1168.05963(58)		
C_A	854.778853(48)			934.93044(83)		
ΔA_E	-0.19428(63)			-0.214(18)		
ΔB_E	-0.000272(63)			0*		
ΔC_E	-0.002064(42)			-0.00431(67)		
A_0	2002.32424(80)[d]	2002.324324(1)	1983.555	1795.819(22)[d]	1795.8822(68)	1778.104
B_0	1155.65465(12)[d]	1155.656893(32)	1147.855	1168.05963(58)[d]	1168.06270(44)	1159.155
C_0	854.777477(76)[d]	854.775228(32)	847.588	934.9276(13)[d]	934.921628(52)	927.172
$D_J \cdot 10^3$	0.05999(36)	0.06101(22)	0.0600	0.171(27)	0.091(17)	0.0885
$D_K \cdot 10^3$	-0.0026*	-0.091(20)	-0.0026	-0.1283*	-0.1283*	-0.1283
$D_{JK} \cdot 10^3$	0.1918(40)	0.1884(33)	0.1963	0.2421*	0.2421*	0.2421
$d_1 \cdot 10^3$	-0.01729(25)	-0.01803(16)	-0.0177	0.0125*	0.0125*	0.0125
$d_2 \cdot 10^3$	0.00008*	0.00008*	0.00008	0.0070*	0.0070*	0.0070
3/2 $\chi_{aa,1}$	-24.3364(54)	-24.3278(42)	-24.40	29.8349(64)	29.8390(45)	28.57
3/2 $\chi_{aa,2}$	47.2728(63)	47.2696(47)	46.21	29.8349(64)	29.8390(45)	28.57
¼ ($\chi_{bb,1} - \chi_{cc,1}$)	-11.1217(24)	-11.1226(18)	-11.03	-15.8402(23)	-15.8418(16)	-15.76
¼ ($\chi_{bb,2} - \chi_{cc,2}$)	-22.2806(23)	-22.2775(17)	-22.02	-15.8402(23)	-15.8418(16)	-15.76
$\chi_{ab,1}$	52.94(36)	53.76(29)	52.98	39.85(27)	38.86(19)	38.38
$\chi_{ab,2}$	-26.27(47)	-27.11(37)	-26.73	-39.85(27)	-38.86(19)	-38.38
$\chi_{ac,1}$	-22.18*	-23.37(59)	-22.18	18.75(52)	19.29(36)	18.87
$\chi_{ac,2}$	-8.83*	-9.0(11)	-8.83	18.75(52)	19.29(36)	18.87
$\chi_{bc,1}$	22.81(23)	22.68(20)	21.32	-37.758(94)	-38.303(61)	-36.65
$\chi_{bc,2}$	-33.23(17)	-33.28(13)	-31.79	37.758(94)	38.303(61)	36.65
D_a	8.6281(11)			9.3158(39)		
D_b	0.47415[#]			0*		
D_c	0.97345(13)			1.069(50)		
F_0/GHz		158.6[$]	158.1		158.6[$]	158.1
V_3/cm^{-1}		349.667(22)	339		335.611(56)	326
δ/°		14.908(60)	15.7		13.83(17)	14.2
ϵ/°		96.4(22)	109.8		90*	90
Lines *A* / Lines *E*	548/430	548/430		117 / 109	117/109	
σ_A / σ_E / σ_{Total} in kHz	12/14/13	10/10/10		10/12/11	8/8/8	
$\Delta G^{\ominus}_{m,,298K}$ in kJ/mol	0		0	≈ -1.4 ± 1.1		1.01[†]

d – Derived parameters. * – Fixed on quantum chemical prediction. [#] – Fixed on value predicted from *XIAM* fits in conjunction with CAM-B3LYP-D3BJ/aVTZ predicted geometric changes and the *Mathieu* program. [$] – Fixed on value of n-$C_4F_9OCH_3$ in Ref. [22]. [†] -$\frac{N_{Cs}}{0.5N_{C_1}} = \exp(\Delta G^{\ominus}_{m,,298K}/-RT) = 0.66$ and $\frac{N_{Cs}}{NC_1} = 0.33$ with the factor of one half originating from the two fold degeneracy of C_1 and the resulting equilibria of C_S-conformer and two C_1-enantiomers - This value is in discrepancy with our experimental estimate 0.88 ± 0.30.

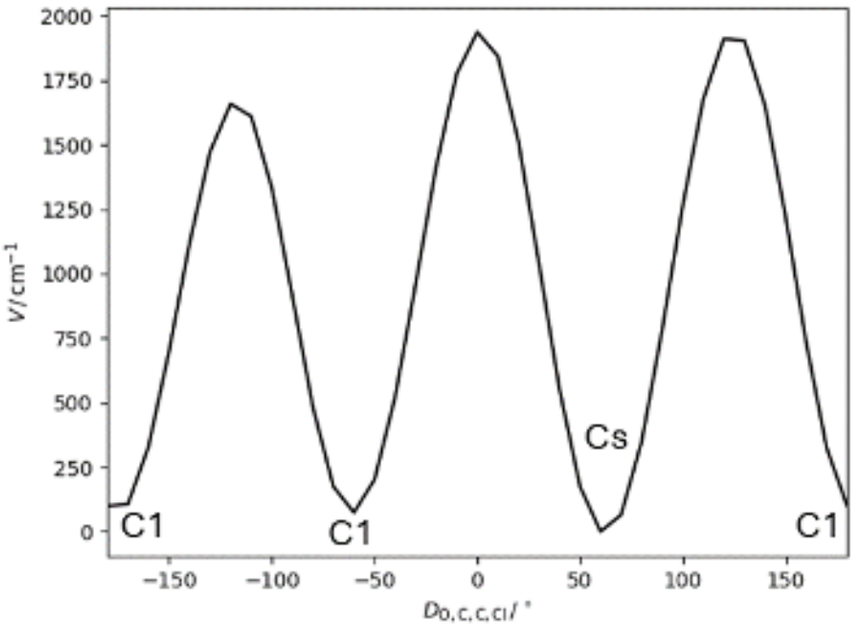

Fig. 4: Potential energy (V) dependence of the dihedral angle $D_{O,C,C,Cl}$, converting between the two equivalent *gauche-trans* C_1-enantiomers and the *trans-trans* C_S-conformer calculated at the CAM-B3LYP-D3(BJ)/aug-cc-pVTZ level.

IV. CONCLUSIONS

This study presents the first high-resolution rotational analysis of methoxyflurane, marking the first complete analysis of a C_1-symmetric molecule with two strong quadrupolar nuclei and internal rotation. Previous low resolution studies on methoxyflurane were hindered by the combined fine and hyperfine structures of two conformers and multiple isotopologues, as well as the absence of spectral fitting codes implementing the required quantum mechanical models.

In this context, this study also represents a methodological advancement in spectroscopic fitting techniques for handling the simultaneous presence of two strong quadrupole coupling nuclei and internal rotation. This development enabled the successful fitting of four isotopologues of the *gauche-trans* C_1-conformer and three isotopologues of the *trans-trans* C_S-symmetric conformer of methoxyflurane. We accomplished this in two stages: first, by using a workaround routine with *SPFIT/SPCAT* to handle two nuclear quadrupole couplings with internal rotation, achieving near-experimental accuracy; and second, by developing the new spectral fitting code *XIAM-2NQ*, which reproduces experimental frequencies with experimental accuracy.

Subsequently, we examine the relative conformer population ratios in the jet, using relative intensities to derive the Gibbs free energy difference between the two conformers. The experiment confirmed the

C_1-symmetric conformer to be more abundant, due to its two-fold degeneracy (two enantiomers), providing empirical reference for further computational studies.

The results offer new perspectives for future studies of related molecules and emphasize the detailed structural information resulting from the unique frequency resolution of rotational spectroscopy, routinely achieving isotopic and conformational discrimination. The combination of spectroscopy with quantum chemical calculations provides the arguably most effective tool for the investigation of gas-phase molecules.

SUPPLEMENTARY MATERIAL

Two supplementary files and one folder are uploaded with this document:

1) 'PICKETT.pdf' contains additional information on the applied two-step procedure using *SPFIT* as well as a complete line list including tentative assignments.
2) 'RELATIVE_POPULATION.pdf' contains details on how the relative populations of C_1- and C_S-conformer were determined from the experimental spectrum.
3) 'XIAM_FITS.zip' contains all *XIAM-2NQ* input and output files. The *XIAM-2NQ* source code and a compiled executable are available on the https://github.com/SvenHerbers/XIAM-2NQ

ACKNOWLEDGEMENTS

During the preparation of this manuscript, we received private communication from K. Vávra regarding his ongoing development of a new, yet unpublished general fitting code intended to also address quadrupole coupling and internal rotation, efforts which we would like to acknowledge here.

P.B., M.L., and J.-U.G. thank the DFG and the Land Niedersachsen for funding, as well as the LUIS Cluster-Team for their support.

W.L. and A.L. acknowledge funding from the European Regional Development Fund (ERDF) and the *Ministerio de Ciencia e Innovación* under Grant No. PID2021-125015NB-I00 and the *Junta de Castilla y León* and ERDF for Grant INFRARED IR2021-UVa13.

DATA AVAILABILITY STATEMENT

The data supporting the findings of this study are available within the article and its supplementary material. The Python scripts used to run the two-step procedure with *SPFIT* are available from S.H. The most recent version of *XIAM-2NQ* is available from S.H. and on GitHub at https://github.com/SvenHerbers/XIAM-2NQ

CONFLICT OF INTEREST

The authors declare no conflicts of interest.

AUTHOR CONTRIBUTIONS

- **Sven Herbers**: Software (lead); formal analysis (lead); writing – original draft (equal); writing – review & editing (equal).
- **Wenqin Li**: Investigation (lead); formal analysis (supporting); writing – review & editing (equal).
- **Philipp Buschmann**: Investigation (supporting); formal analysis (supporting); writing – review & editing (equal).
- **Meng Li**: Investigation (supporting); formal analysis (supporting); writing – review & editing (equal).
- **Alberto Lesarri**: Writing – original draft (equal); writing – review & editing (equal); funding acquisition (equal); project administration (equal); supervision (equal).
- **Jens-Uwe Grabow**: Writing – review & editing (equal); Funding acquisition (equal); project administration (equal); supervision (equal).

REFERENCES

[1] D. Belelli, M. Pistis, J.A. Peters, and J.J. Lambert, "General anaesthetic action at transmitter-gated inhibitory amino acid receptors," Trends Pharmacol Sci **20**(12), 496–502 (1999).
[2] H.C. Hemmings, M.H. Akabas, P.A. Goldstein, J.R. Trudell, B.A. Orser, and N.L. Harrison, "Emerging molecular mechanisms of general anesthetic action," Trends Pharmacol Sci **26**(10), 503–510 (2005).
[3] N.P. Franks, "General anaesthesia: from molecular targets to neuronal pathways of sleep and arousal," Nat Rev Neurosci **9**(5), 370–386 (2008).
[4] R.L. Macdonald, and R.W. Olsen, "GABAA Receptor Channels," Annu Rev Neurosci **17**(1), 569–602 (1994).
[5] S. Cull-Candy, S. Brickley, and M. Farrant, "NMDA receptor subunits: diversity, development and disease," Curr Opin Neurobiol **11**(3), 327–335 (2001).
[6] N.P. Franks, and E. Honoré, "The TREK K2P channels and their role in general anaesthesia and neuroprotection," Trends Pharmacol Sci **25**(11), 601–608 (2004).
[7] A.J. Patel, E. Honoré, F. Lesage, M. Fink, G. Romey, and M. Lazdunski, "Inhalational anesthetics activate two-pore-domain background K+ channels," Nat Neurosci **2**(5), 422–426 (1999).
[8] A.A. Bhattacharya, S. Curry, and N.P. Franks, "Binding of the General Anesthetics Propofol and Halothane to Human Serum Albumin," Journal of Biological Chemistry **275**(49), 38731–38738 (2000).
[9] R. Liu, P.J. Loll, and R.G. Eckenhoff, "Structural basis for high-affinity volatile anesthetic binding in a natural 4-helix bundle protein," The FASEB Journal **19**(6), 567–576 (2005).
[10] A. Lesarri, A. Vega-Toribio, R.D. Suenram, D.J. Brugh, and J.-U. Grabow, "The conformational landscape of the volatile anesthetic sevoflurane," Physical Chemistry Chemical Physics **12**(33), 9624–9631 (2010).
[11] A. Lesarri, A. Vega-Toribio, R.D. Suenram, D.J. Brugh, D. Nori-Shargh, J.E. Boggs, and J.-U. Grabow, "Structural evidence of anomeric effects in the anesthetic isoflurane," Physical Chemistry Chemical Physics **13**(14), 6610–6618 (2011).
[12] S.T. Shipman, and B.H. Pate, "New Techniques in Microwave Spectroscopy," in *Handbook of High-Resolution Spectroscopy*, edited by F. Merkt and M. Quack, (John Wiley & Sons, Ltd, New York, 2011), pp. 801–828.
[13] C. Pérez, E. Caballero-Mancebo, A. Lesarri, E.J. Cocinero, I. Alkorta, R.D. Suenram, J.-U. Grabow, and B.H. Pate, "The Conformational Map of Volatile Anesthetics: Enflurane Revisited," Chemistry - A European Journal **22**(28), 9804–9811 (2016).
[14] I. Uriarte, P. Écija, L. Spada, E. Zabalza, A. Lesarri, F.J. Basterretxea, J.A. Fernández, W. Caminati, and E.J. Cocinero, "Potential energy surface of fluoroxene: Experiment and theory," Physical Chemistry Chemical Physics **18**(5), 3966–3974 (2016).
[15] A. Lesarri, S.T. Shipman, J.L. Neill, G.G. Brown, R.D. Suenram, L. Kang, W. Caminati, and B.H. Pate, "Interplay of phenol and isopropyl isomerism in propofol from broadband chirped-pulse microwave spectroscopy," J Am Chem Soc **132**(38), 13417–13424 (2010).
[16] A. Insausti, C. Calabrese, M. Parra, I. Usabiaga, M. Vallejo-López, P. Écija, F.J. Basterretxea, J.-U. Grabow, W. Caminati, A. Lesarri, and E.J. Cocinero, "Conformational impact of aliphatic side chains in local anaesthetics: benzocaine, butamben and isobutamben," Chemical Communications **56**, 6094–6097 (2020).
[17] R.C. Terrell, and D.S. Warner, "The Invention and Development of Enflurane, Isoflurane, Sevoflurane, and Desflurane," Anesthesiology **108**(3), 531–533 (2008).
[18] R.I. Mazze, and S.N. Raja, "Methoxyflurane Revisited," Anesthesiology **105**(4), 843–846 (2006).
[19] R.I. Mazze, J.R. Trudell, and M.J. Cousins, "Methoxyflurane Metabolism and Renal Dysfunction," Anesthesiology **35**(3), 247–252 (1971).

[20] C. Jephcott, J. Grummet, N. Nguyen, and O. Spruyt, "A review of the safety and efficacy of inhaled methoxyflurane as an analgesic for outpatient procedures," Br J Anaesth **120**(5), 1040–1048 (2018).
[21] Y.S. Li, and J.R. Durig, "Microwave, infrared and Raman spectra, conformational stability and vibrational assignment of methoxyflurane," J Mol Struct **81**(3–4), 181–194 (1982).
[22] G.S. Grubbs, and S.A. Cooke, "Structure and Barrier to Methyl Group Internal Rotation for $(CF_3)_2CFCF_2OCH_3$ and Its Isomer n-$C_4F_9OCH_3$ (HFE-7100)," J Phys Chem A **115**(6), 1086–1091 (2011).
[23] E. Antonelli, E. Gougoula, N.R. Walker, M. Schwell, H.V.L. Nguyen, and I. Kleiner, "A global rho-axis method for fitting asymmetric tops with one methyl internal rotor and two 14N nuclei: Application of BELGI-2N to the microwave spectra of four methylimidazole isomers," J Chem Phys **160**(21), (2024).
[24] J.H. Westerfield, and S.E. Worthington-Kirsch, "westerfit: A new program for spin–torsion–rotation spectra," J Mol Spectrosc **404**, 111928 (2024).
[25] S. Herbers, "XIAM-NQ: Implementation of exact quadrupole coupling," J Mol Spectrosc **405**, 111950 (2024).
[26] J.-U. Grabow, "Fourier Transform Microwave Spectroscopy Measurement and Instrumentation," in *Handbook of High-Resolution Spectroscopy*, edited by F. Merkt and M. Quack, (John Wiley & Sons, Ltd, New York, 2011), pp. 723–799.
[27] J.-U. Grabow, W. Stahl, and H. Dreizler, "A multioctave coaxially oriented beam-resonator arrangement Fourier-transform microwave spectrometer," Review of Scientific Instruments **67**(12), 4072–4084 (1996).
[28] T. Yanai, D.P. Tew, and N.C. Handy, "A new hybrid exchange–correlation functional using the Coulomb-attenuating method (CAM-B3LYP)," Chem Phys Lett **393**(1–3), 51–57 (2004).
[29] E.R. Johnson, and A.D. Becke, "A post-Hartree–Fock model of intermolecular interactions," J Chem Phys **123**(2), (2005).
[30] E.R. Johnson, and A.D. Becke, "A post-Hartree-Fock model of intermolecular interactions: Inclusion of higher-order corrections," J Chem Phys **124**(17), 174104 (2006).
[31] H. Schröder, A. Creon, and T. Schwabe, "Reformulation of the D3(Becke-Johnson) Dispersion Correction without Resorting to Higher than C6 Dispersion Coefficients," J Chem Theory Comput **11**(7), 3163–3170 (2015).
[32] T.H. Dunning, "Gaussian basis sets for use in correlated molecular calculations. I. The atoms boron through neon and hydrogen," J Chem Phys **90**(2), 1007–1023 (1989).
[33] M.J. Frisch, G.W. Trucks, H.B. Schlegel, G.E. Scuseria, M.A. Robb, J.R. Cheeseman, G. Scalmani, V. Barone, G.A. Petersson, H. Nakatsuji, X. Li, M. Caricato, A. V. Marenich, J. Bloino, B.G. Janesko, R. Gomperts, B. Mennucci, H.P. Hratchian, J. V. Ortiz, A.F. Izmaylov, J.L. Sonnenberg, Williams, F. Ding, F. Lipparini, F. Egidi, J. Goings, B. Peng, A. Petrone, T. Henderson, D. Ranasinghe, V.G. Zakrzewski, J. Gao, N. Rega, G. Zheng, W. Liang, M. Hada, M. Ehara, K. Toyota, R. Fukuda, J. Hasegawa, M. Ishida, T. Nakajima, Y. Honda, O. Kitao, H. Nakai, T. Vreven, K. Throssell, J.A. Montgomery Jr., J.E. Peralta, F. Ogliaro, M.J. Bearpark, J.J. Heyd, E.N. Brothers, K.N. Kudin, V.N. Staroverov, T.A. Keith, R. Kobayashi, J. Normand, K. Raghavachari, A.P. Rendell, J.C. Burant, S.S. Iyengar, J. Tomasi, M. Cossi, J.M. Millam, M. Klene, C. Adamo, R. Cammi, J.W. Ochterski, R.L. Martin, K. Morokuma, O. Farkas, J.B. Foresman, and D.J. Fox, "Gaussian 16, rev. C.01," (2016).
[34] H.M. Pickett, "The fitting and prediction of vibration-rotation spectra with spin interactions," J Mol Spectrosc **148**(2), 371–377 (1991).
[35] J.K.G. Watson, "Aspects of Quartic and Sextic Centrifugal Effects on Rotational Energy Levels," in *Vibrational Spectra and Structure, Vol. 6*, edited by J.R. Durig, (Elsevier B.V., Amsterdam, 1977), pp. 1–89.
[36] H.P. Benz, A. Bauder, and Hs.H. Günthard, "Exact quadrupole interaction energies in rotational spectra," J Mol Spectrosc **21**(1–4), 156–164 (1966).

[37] D.R. Herschbach, "Calculation of Energy Levels for Internal Torsion and Over-All Rotation. III," J Chem Phys **31**(1), 91–108 (1959).
[38] H. Hartwig, and H. Dreizler, "The Microwave Spectrum of trans-2,3-Dimethyloxirane in Torsional Excited States," Zeitschrift Für Naturforschung A **51**(8), 923–932 (1996).
[39] S. Herbers, O. Zingsheim, H.V.L. Nguyen, L. Bonah, B. Heyne, N. Wehres, and S. Schlemmer, "Internal rotation arena: Program performances on the low barrier problem of 4-methylacetophenone," J Chem Phys **155**(22), (2021).
[40] O.C. Gorton, C.W. Johnson, C. Jiao, and J. Nikoleyczik, "dmscatter: A fast program for WIMP-nucleus scattering," Comput Phys Commun **284**, 108597 (2023).
[41] S. Herbers, "XIAM-2NQ repository" (2025). https://github.com/SvenHerbers/XIAM-2NQ
[42] W. Caminati, and J.-U. Grabow, "Microwave Spectroscopy: Molecular Systems," in *Frontiers of Molecular Spectroscopy*, edited by J. Laane, (Elsevier, Amsterdam, 2009), pp. 455–552.
[43] N.A. Seifert, I.A. Finneran, C. Pérez, D.P. Zaleski, J.L. Neill, A.L. Steber, R.D. Suenram, A. Lesarri, S.T. Shipman, and B.H. Pate, "AUTOFIT, an automated fitting tool for broadband rotational spectra, and applications to 1-hexanal," J Mol Spectrosc **312**, 13–21 (2015).
[44] R.S. Ruoff, T.D. Klots, T. Emilsson, and H.S. Gutowsky, "Relaxation of conformers and isomers in seeded supersonic jets of inert gases," J Chem Phys **93**(5), 3142–3150 (1990).